Available online at www.sciencedirect.com

SciVerse ScienceDirect

Ceramics International 39 (2013) 4507–4512

CERAMICS INTERNATIONAL

www.elsevier.com/locate/ceramint

Ageing effect on electrical properties of the oxyapatite/ Nd_2NiO_4 interface

Sami Chefi[a,*], Messoud Kahlaoui[a], Abdwaheb Inoubli[a], Adel Madani[a], Abdelkader Hammou[b]

[a]*Laboratoire de Physique des Matériaux, Faculté des Sciences de Bizerte, Zarzouna 7021, Tunisia*

[b]*Laboratoire d'Electrochimie et de Physico-chimie des Matériaux et des Interfaces (INPG, CNRS et UJF) 1130, rue de la Piscine, B.P75, 38402 Saint Martin d'Hères CEDEX, France*

Received 16 October 2012; received in revised form 15 November 2012; accepted 16 November 2012
Available online 23 November 2012

Abstract

In the present work, the influence of the ageing process on the electrical properties of the oxyapatite $La_{10}Si_{5.5}Al_{0.5}O_{26.75}$/ Nd_2NiO_4 interface is studied. Samples were submitted to a thermal treatment at 1200 °C in air for different periods. X-ray diffraction and electron microscopy micrographs show a significant morphological change occurring in both electrolyte and cathode components after 309 h. An important degradation of electrical properties versus time was observed. Conductivity results show an increase of the activation energy and a decrease of the pre-exponential factor for the bulk and the grain boundary of the $La_{10}Si_{5.5}Al_{0.5}O_{26.75}$ electrolyte. Diffusion processes operating during the heat treatments might be involved to explain this behavior. Furthermore, an increase of the electrode resistance by a factor of 5 is observed. Finally, it is worth mentioning that no degradation of this interface was revealed after several periods of heat treatment at 1000 °C in air.

Keywords: B. Impedance spectroscopy; C. Ageing; C. Ionic conductivity; D. Oxyapatites

1. Introduction

Many authors [1–5] have already reported detailed studies showing the good electrical performances of oxyapatites. The stoichiometry of these materials is pretty easy to control, and their conductivity can be significantly improved. Moreover they offer better electrical properties in comparison with the classical Yttria Stabilized Zirconia (YSZ) at intermediate temperature that makes them very attractive as electrolyte in the Solid Oxide Fuel Cell (SOFC) area. Among all the conducting oxyapatites, $La_{10}Si_{5.5}Al_{0.5}O_{26.75}$ composition seems to be the most promising material. However, before envisaging any industrial application, stability of electrical properties with time mainly at the cathode/electrolyte interface should be investigated. It is a common knowledge that the development of metal oxides based cathode materials in SOFC should take into account of their chemical and structural stability versus time. Several factors can be considered as responsible for instability: temperature, oxygen partial pressure, formation of new impedant phases at the electrolyte/cathode interface, contact losses between the active materials of the cell. All these factors can lead to the decrease of the cell's performance with time.

Oxyapatites with general formula $La_{10}Si_{6-x}Al_xO_{26.75}$ is currently under study to be used for the development of the SOFC. Moreover, the manufacturing processes of the SOFC imply the deposition of the Nd_2NiO_4 cathode. Furthermore, it has been proved recently [6] that association between the apatite electrolyte and the nickelate cathodes, exhibit an important results in terms of chemical stability and high conductivity at 700 °C.

The main objective of the present work is to measure the variation of bulk and grain boundary conductivities of $La_{10}Si_{5.5}Al_{0.5}O_{26.75}$ versus time. Let us recall that $La_{10}Si_{5.5}Al_{0.5}O_{26.75}$ corresponds to a maximum in conductivity in the $La_{10}Si_{6-x}Al_xO_{26.75}$ family [1]. Thermal

*Corresponding author. Tel.: +216 50681732; fax: +216 72590566.
E-mail address: chefisami@yahoo.fr (S. Chefi).

0272-8842/$ - see front matter © 2012 Elsevier Ltd and Techna Group S.r.l. All rights reserved.
http://dx.doi.org/10.1016/j.ceramint.2012.11.046

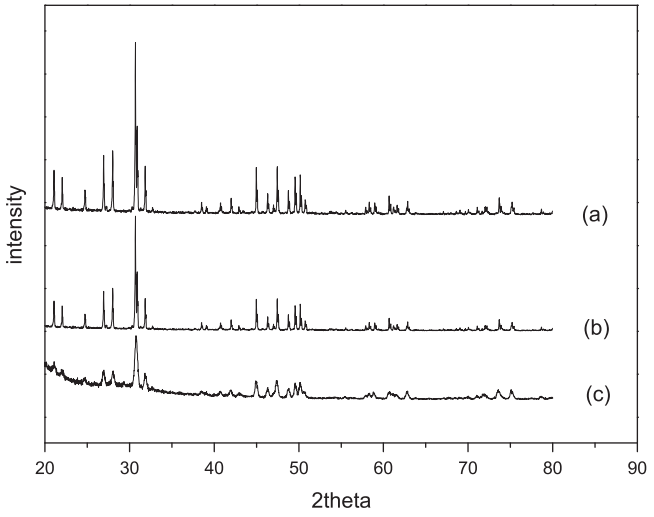

Fig. 1. XRD spectra of $La_{10}Si_{5.5}$ $Al_{0.5}O_{26.75}$, (a) as prepared, after heat treatment for 309 h at: (b) 1000 °C and (c) 1200 °C in air.

degradation of the Nd_2NiO_4, one of the most promising cathode materials, was also studied in the same conditions resulting from thermal treatment of the interface $La_{10}Si_{5.5}Al_{0.5}O_{26.75}$/ Nd_2NiO_4. To increase the speed of degradation, we have chosen to study the ageing effect at temperature nearby1200 °C.

2. Experimental procedure

High purity La_2O_3, SiO_2 (Prolabo 99.9%) and Al_2O_3 (Baikalox 99.9%) powders were used to prepare the oxyapatites samples. Before weighting, La_2O_3 and SiO_2 powders were dried at 1000 °C and 1200 °C respectively for 1 h. The powders with stoichiometric ratios were mixed, ground with ethanol in equal quantity and calcinated at 1500 °C for 2 h [7]. The calcinated powders were ground using attrition procedure and uniaxially pressed as pellets. Finally, these pellets were isostatically pressed at 2.5 kbar and sintered at 1600 °C for 3 h in air.

The cathode material Nd_2NiO_4 was prepared using the usual nitrate–citrate route [8]. A stoichiometric mixture of Nd_2O_3 (Prolabo 99.9%) and NiO (Aldrich 99.9%) was dissolved in nitric acid solution. After that, citric acid solution was added. The solution was evaporated leading to a submicronic particles mixture of precursors. Several annealings at 1000 °C for 12 h were carried out to obtain the final powder. A slurry was prepared by introducing the Nd_2NiO_4 powder in a solution containing ethanol, terpineol, PVP (polyvinylpyrrolidone) and PVB (Polyvinylbutyral). For electrical measurements, a symmetrical cell was prepared by painting both sides of the oxyapatite disk with the Nd_2NiO_4 slurry. In order to improve the electrical contacts, samples were pressed between two platinum grids. In order to investigate the influence of the ageing processes on the properties of the studied materials, the samples were submitted to a thermal treatment at 1200 °C for 309 h. Ageing treatment was performed in air at 1200 °C during different cycles. After each thermal treatment, the cell was cooled down to 200 °C and impedance measurements were performed up to 700 °C. Electrical properties were measured using a Hewlett Packard HP 4192 analyzer in the frequency range 5 Hz–13 MHz and an Autolab analyzer in the frequency range 10 mHz–1 MHz. Impedance spectra was recorded after every treatment, analyzed and fitted using the Z view software.

To determine the samples crystallographic structure, X-ray diffraction analysis (XRD) was performed at a room temperature with a Pan Analytical diffractometer using Cu Kα_1 radiation. Microscopic examinations were performed using a Jeol JSM.6400 scanning electron microscope.

3. Results and discussion

3.1. Microstructural characterization

Diffraction patterns of oxyapatite sample before and after heat treatment (309 h, 1200 °C) are shown in Fig. 1. The crystalline phases were identified from a comparison of the registered patterns with the international center for diffraction data (ICDD) powder diffraction files (PDF). Both samples of $La_{10}Si_{5.5}$ $Al_{0.5}O_{26.75}$ show a hexagonal structure and no lines of secondary phase are observed. Diffraction patterns associated to the electrolyte show a decrease of the relative intensity of the diffraction peaks of about 70% after heat treatment, compared to that of the as prepared electrolyte. This intensity decrease could be explained by a loss in crystallinity or in symmetry. A similar behavior was observed in the literature with YSZ [9,10]. Fig. 2b shows the XRD patterns of the cathode/electrolyte interface after 309 h heat treatment at 1200 °C. The typical reflections of oxyapatite $La_{10}Si_{5.5}Al_{0.5}O_{26.75}$ and cathode material Nd_2NiO_4 are present. Furthermore, diffraction peaks at $2\theta = 31.79°$ and 46.48° are indicative of

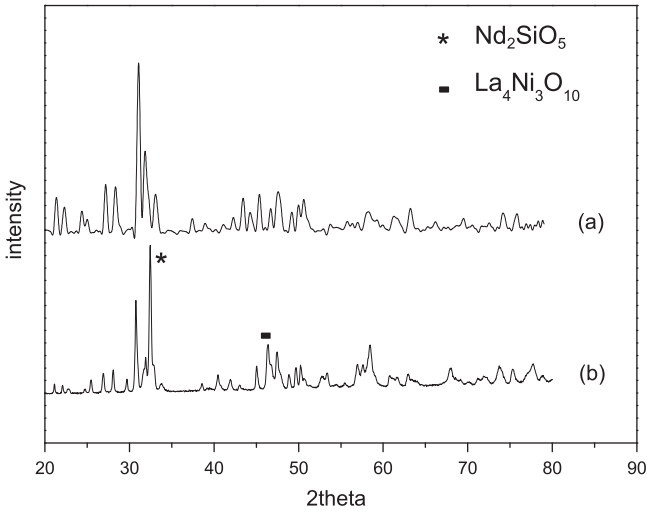

Fig. 2. XRD patterns of $La_{10}Si_{5.5}Al_{0.5}O_{26.75}/Nd_2NiO_4$ interface after heat treatment for 309 h in air at: (a) 1000 °C and (b) 1200 °C.

the X-ray reflections typical respectively of Nd_2SiO_5 (ICDD 00-040-0284) and $La_4Ni_3O_{10}$ (ICDD 00-035-1242) phases.

However, it is worth to mention that not all the reactivities were observed between cathode and electrolyte materials at 1000 °C after a heat treatment of more than 300 h in air (Fig. 2a). Such result has already been observed in literature [6], where it is verified that no chemical reactivity is detectable between the apatite electrolyte, i.e., $La_9Sr_1Si_6O_{26.5}$, and Nd-deficient nickelate, i.e. $Nd_{1.95}NiO_{4+\delta}$, over more than one month, even at temperatures as high as 920 °C.

3.2. Electrolyte electrical properties

Fig. 3 shows the variation of the impedance diagrams recorded at 261 °C in air as function of the heat treatment time. A very important increase of the electrolyte resistance is observed. Bulk conductivities σ_b and grain boundary conductivitiesσ_{gb} were calculated using the following relation:

$$\sigma_i = \frac{1}{R_i}\frac{L}{S} \tag{1}$$

R_i (i=bulk, grain boundary) is the resistance obtained from impedance diagrams and S and L are the area and the thickness of the sample respectively. The Arrhenius plots of the electrical conductivity σ_i are shown in Figs. 4 and 5 for bulk and grain boundary contributions respectively. The observed linear behavior allows to express the electrical conductivity as follows:

$$\sigma T = A\exp\left(-\frac{E_a}{kT}\right) \tag{2}$$

where E_a is the activation energy, k is the Boltzmann constant and A is the pre-exponential factor whose expression in the usual treatment [11–13] of ionic conductivity is:

$$\frac{A = 2Ce^2\upsilon l^2}{k} \tag{3}$$

where υ is the jump frequency, l is the interatomic jump distance, e is the electron charge and C is a constant

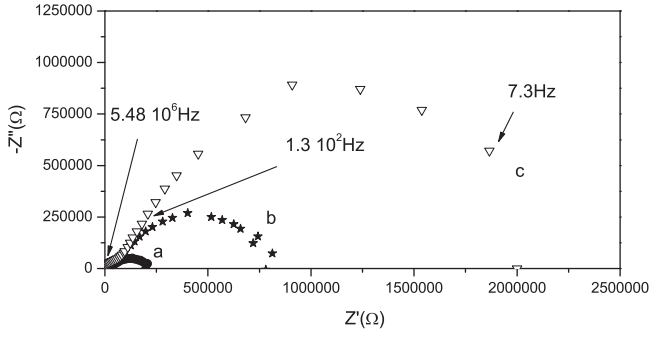

Fig. 3. Variation of impedance spectra recorded at 261 °C versus time of heat treatment at 1200 °C of $La_{10}Si_{5.5}$ $Al_{0.5}O_{26.75}$ in air: (a) t=0, (b) t=92 h and (c) t=309 h.

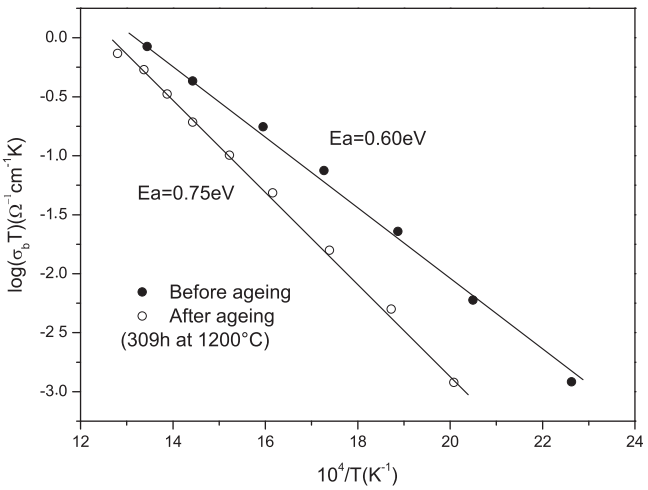

Fig. 4. Temperature dependence of the bulk conductivity of oxyapatite in air.

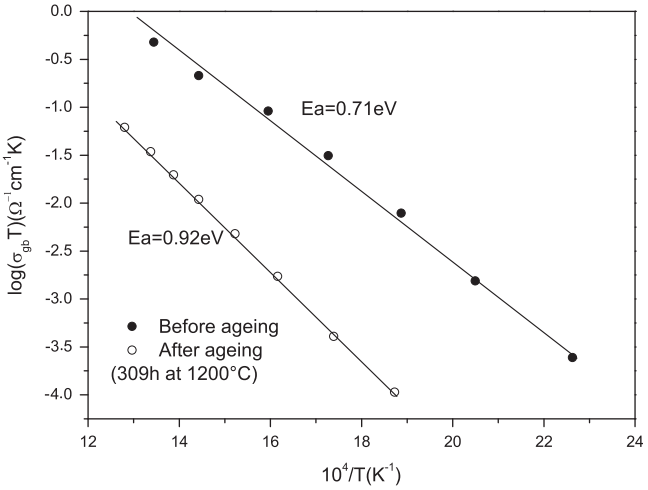

Fig. 5. Temperature dependence of the grain boundary conductivity of oxyapatite in air.

related to concentration of the mobile oxide ion and to geometric and entropy effects associated to the charge carrier.

Conductivity results are analyzed through activation energy and pre-exponential factor variations versus ageing time. Table 1 and Figs. 4 and 5 show the change of the activation energy and the pre-exponential factor resulting from thermal treatment. These two factors act in the same way leading to the decrease of the electrical conductivity. So, after ageing, activation energy increases and the A pre-exponential factor decreases in both bulk and grain boundary. The origin of this difference could be very likely attributed to the composition and/or structure changes revealed by the analysis of the XRD patterns.

In Fig. 6, the variation of the total conductivity ($\sigma_b+\sigma_{gb}$) as a function of ageing time t at 700 °C is shown. These results are in agreement with those presented in a previous work [1]. One observes an important variation of conductivity, the decrease being more than a factor two of

Table 1
Variation of the pre-exponential factor A after a thermal treatment for 309 h at 1200 °C in air.

	Before ageing	After ageing
Pre-exponential factor A (bulk)	3.85×10^4	3.36×10^4
Pre-exponential factor A (grain boundary)	7.23×10^4	6.54×10^4

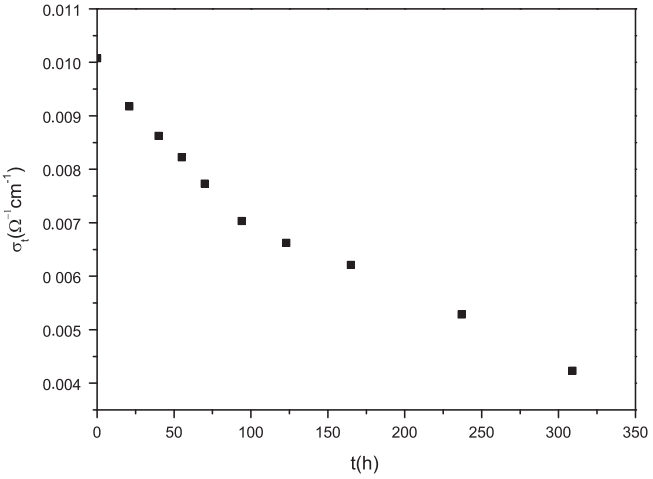

Fig. 6. Variation of total conductivity as a function of ageing time in air at 700 °C.

magnitude. Furthermore, it can be seen that, at the beginning of the ageing, the electrical conductivity decreases rapidly with the ageing time; but after 100 h of thermal treatment, this variation becomes less fast.

In the following, bulk and grain boundary conductivities are treated in considering their relative changes defined as $(\sigma_o - \sigma_t)/\sigma_o$. σ_o and σ_t refer respectively to the initial conductivity and the conductivity measured after a heating treatment time t. Fig. 7 shows the variation of $(\sigma_o - \sigma_t)/\sigma_o$ versus $t^{1/2}$. A linear variation is clearly observed for the first 100 h. For the later stage, no significant evolution is detected. Conversely, for grain boundary, Fig. 8 shows a linear variation of $(\sigma_o - \sigma_t)/\sigma_o$ versus $t^{1/2}$ for the whole investigated time of heat treatment. In addition, a lower slope is observed in comparison with the bulk behavior suggesting a lower kinetics in the grain boundary conductivity change. Assuming that no chemical or structural variations takes place when the sample is cooled down after each heat treatment for impedance measurements, Figs. 7 and 8 indicate that the heat treatment is responsible for a chemical reaction proceeding very likely via an atomic diffusion.

3.3. Cathode electrical properties

The impedance diagrams associated to the electrode response were recorded at 700 °C in air. Their variation with the heat treatment time at 1200 °C in air is shown in Fig. 9. One observes that the electrode resistance is increased by a

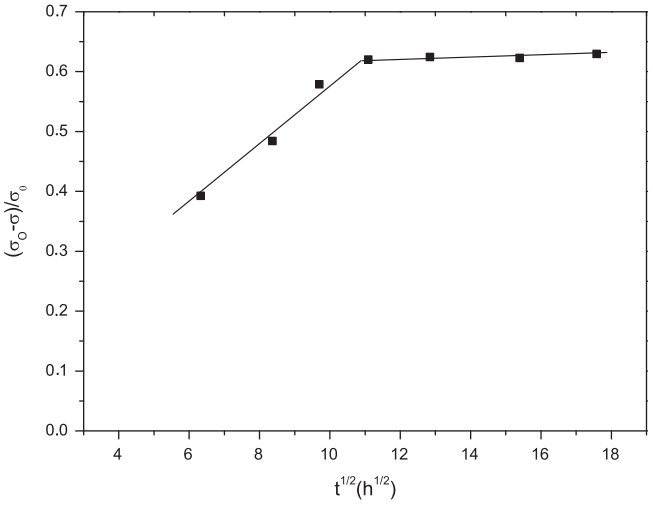

Fig. 7. Variation of the relative change of bulk conductivity of $La_{10}Si_{5.5}Al_{0.5}O_{26.75}$ versus the square root of the aging time $t^{1/2}$.

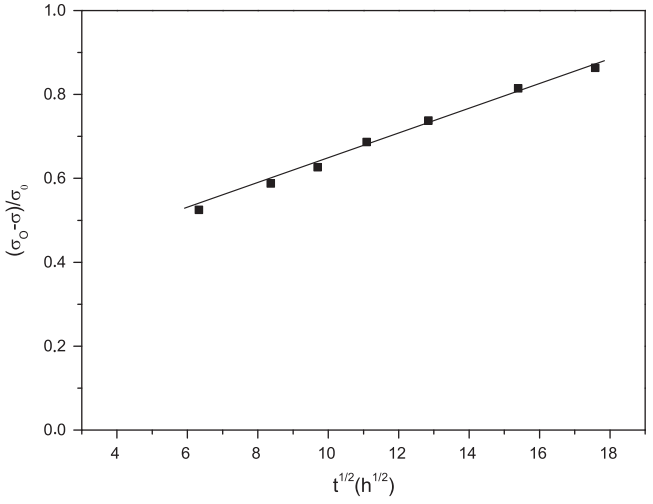

Fig. 8. Variation of the relative change of grain boudary conductivity of $La_{10}Si_{5.5}$ $Al_{0.5}O_{26.75}$ versus the square root of the aging time $t^{1/2}$.

factor 5 for a heat treatment period of 309 h. Here again, the relative electrode conductivity is defined by the following relation $(\sigma_{oE} - \sigma_{tE})/\sigma_{oE}$ and its variation versus $t^{1/2}$ and t is shown in Figs. 10 and 11 respectively. Results suggest that a diffusion-like phenomenon does not chiefly control the electrode process. The increase of the electrode polarization could be attributed to the progressive modification of the interface $La_{10}Si_{5.5}Al_{0.5}O_{26.75}$/ Nd_2NiO_4. This modification might result mainly from the two following factors:

Chemical reaction between the electrolyte and electrode materials leading to their partial degradation and the formation of new phases. XRD analysis revealed the formation of Nd_2SiO_5 and $La_4Ni_3O_{10}$ at the $La_{10}Si_{5.5}Al_{0.5}O_{26.75}$/ Nd_2NiO_4 (see Fig. 12). Usually, chemical reaction kinetic is mainly attributed to the movement of cationic species. In our case, Ni^{2+} diffusion

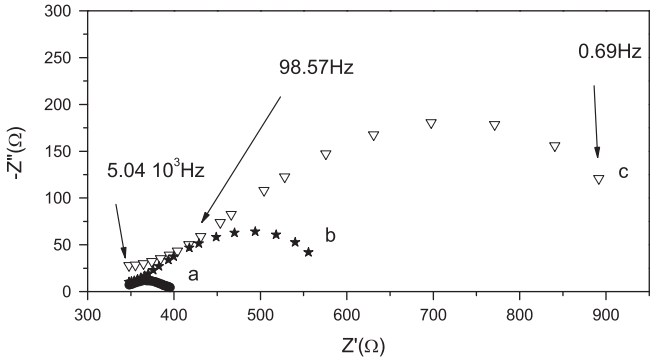

Fig. 9. Influence of the heat treatment (1200 °C) time on the cathode impedance spectra recorded at 700 °C: (a) 0 h, (b) 92 h and (c) 309 h.

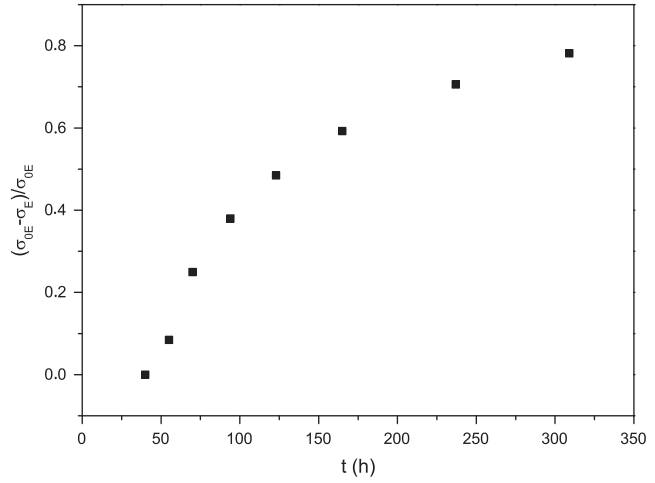

Fig. 10. Variation of the relative electrode conductivity versus the ageing time t.

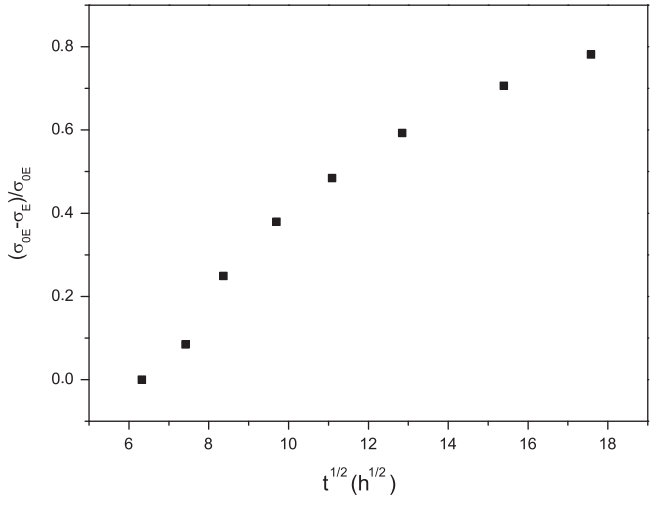

Fig. 11. Variation of the relative electrode conductivity versus the square root of the ageing time $t^{1/2}$.

is very likely the most responsible species for the interfacial chemical reaction due to the lower charge of this cation. The new insulating phases affect the total cell impedance

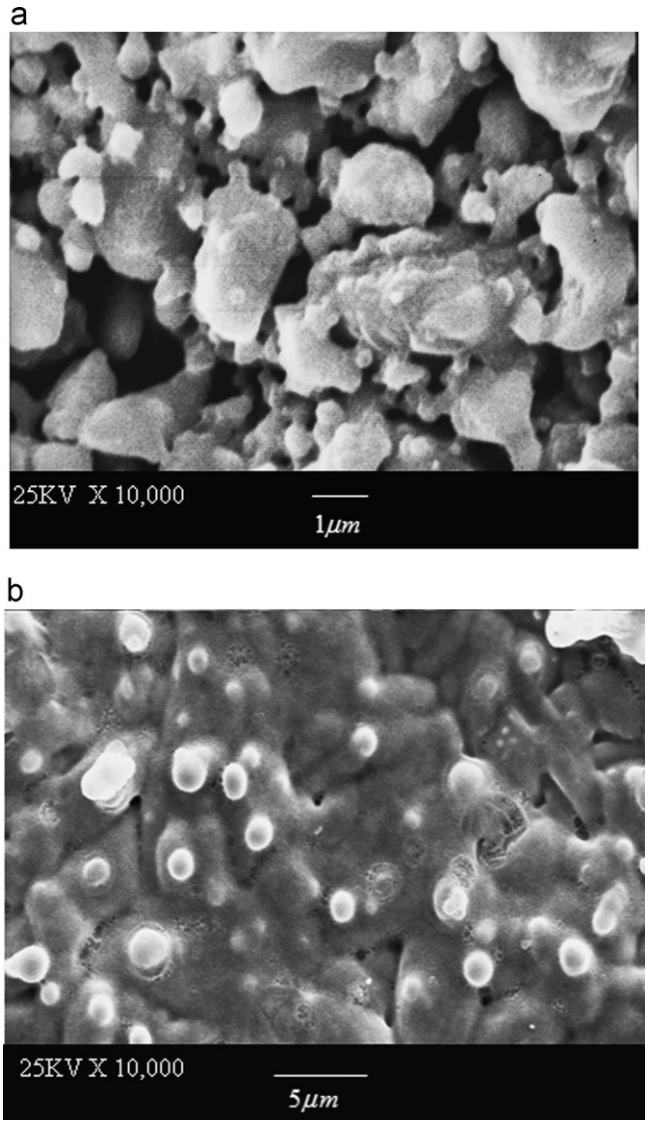

Fig. 12. SEM micrographs of Nd_2NiO_4 layer (a) as deposited; (b) after a working period of 309 h at 1200 °C.

(bulk and grain boundaries) and are responsible of the lower efficiency in terms of electrochemical kinetics at the electrode interface. Our results are not accurate enough to determine the most affected electrochemical process: activation, adsorption, migration … A more detailed study has to be performed to elucidate this point.

The particle size increase, shown in Fig. 12. The mean particle size increases from 1 to 10 μm. That reduces the electrode porosity and the triple point line density where the electrochemical reaction takes place at low current density.

4. Conclusion

In this work, the influence of the ageing of the oxyapatite/Nd_2NiO_4 interface on the electrical properties has been studied. SEM and XRD analysis had shown the degradation of the cathode layer and the formation of impedant

secondary phases on the electrode/electrolyte interface leading to lower electrochemical performances. On the other hand, conductivity results had shown a deterioration of electrical properties through the cell following a $t^{1/2}$ variation law. Such observations let suppose that ageing mechanisms are very likely managed by diffusion processes.

A better understanding of the causes of ageing could suggest new solutions to avoid or, at least, minimize these causes, and consequently improve the performance of the $La_{10}Si_{5.5}Al_{0.5}O_{26.75}/Nd_2NiO_4$ cathode. Work is in progress in order to study more accurately the changes in the structure and composition of the investigated materials, in particular by TEM analysis.

References

[1] S. Chefi, A. Madani, H. Boussetta, C. Roux, A. Hammou, Electrical properties of Al-doped oxyapatites at intermediate temperature, Journal of Power Sources 177 (2008) 464–469.

[2] J.E.H. Sansom, D. Richings, P.R. Slater, A powder neutron diffraction study of the oxide-ion-conducting apatite-type phases, $La_{9.33}Si_6O_{26}$ and $La_8Sr_2Si_6O_{26}$, Solid State Ionics 139 (2001) 205–210.

[3] E.J. Abram, D.C. Sinclair, A.R. West, A novel enhancement of ionic conductivity in the cation-deficient apatite $La_{9.33}(SiO_4)_6O_2$, Journal of Materials Chemistry 11 (2001) 1978–1979.

[4] P.R. Slater, J.E.H. Sansom, The synthesis and characterization of new apatite-type oxide ion conductors, Solid State Phenomena 195 (2003) 90–91.

[5] A.L. Shaula, V.V. Kharton, V.V. Marques, Oxygen ionic and electronic transport in apatite-type La_{10-x} (Si,Al) $_6O_{26\pm\delta}$, Journal of Solid State Chemistry 178 (2005) 2050–2060.

[6] F. Mauvy, C. Lalanne, J.M. Bassat, J.C. Grenier, A. Brisse, A.L. Sauvet, C. Barthet, J. Fouletier, Electrochemical study of the $Nd_{1.95}NiO_{4+\delta}$/ oxide electrolyte interface, Solid State Ionics 180 (2009) 1183–1189.

[7] A. Vincent, Thesis, Tours University, France, 2006.

[8] P. Courty, H. Ajot, C.h. Marcilly, B. Delmon, Oxydes mixtes ou en solution solide sous forme très divisée obtenus par décomposition thermique de précurseurs amorphes, Powder Technology 7 (1973) 21–38.

[9] A.N. Vlasov, M.V. Perfiliev, Ageing of ZrO_2-based solid electrolytes, Solid State Ionics 25 (1987) 245–253.

[10] Z.R. Dai, Z.L. Wang, Y.R. Chen, H.Z. Wu, W.X. Liu, Local ordering of oxygen vacancies in cubic zirconia (ZrO_2) stabilized with yttria (Y_2O_2) and magnesia (MgO) I. Electron diffuse scattering study, Philosophical Magazine A 73 (2) (1996) 415–430.

[11] C. Deportes, M. Duclot, P. Fabry, J. Fouletier, A. Hammou, M. Kleitz, E. Siebert, J.L. Souquet, Electrochimie des Solides, Presses Universitaires de Grenoble. France, 1994.

[12] J. Maier, Transport in electroceramics: micro- and nano-structural aspects, Journal of the European Ceramic Society 24 (6) (2004) 1251–1257.

[13] R.E. Carter, W.L. Roth, in: C.B. Alcock (Ed.), Electromotive Force Measurements in High Temperature Systems, 1968 pp.125–144.